Functionalization of Contacted Carbon Nanotube Forests by Dip Coating for High-Performance Biocathodes

Meenakshi Singh, Hugo Nolan, Maryam Tabrizian, Serge Cosnier, Georg Düsberg, Michael Holzinger

Functionalization of contacted Carbon Nanotube Forests by dip coating for high performing bio-cathodes

Meenakshi Singh[a, b], *Hugo Nolan*[c], *Maryam Tabrizian*[b], *Serge Cosnier*[a], *Georg S. Düsberg*[c, d] *and Michael Holzinger*[a]*

[a]Univ. Grenoble Alpes - CNRS, Département de Chimie Moléculaire, UMR 5250, F-38000 Grenoble, France.

[b]McGillUniversity, Biomat'X Research Laboratories, Dept. of Biomedical Engineering and Faculty of Dentistry, Montréal, Canada.

[c]School of Chemistry, Centre for Research on Adaptive Nanostructures and Nanodevices (CRANN) and Advanced Materials Bio-Engineering Research Centre (AMBER), Trinity College, Dublin 2, Ireland.

[d]Universität der Bundeswehr, München, Neubiberg 85579, Germany.

ABSTRACT. This work focuses on the use of electrically contacted carbon nanotubes forests as an electrode material for the bioelectrocatalytic reduction of oxygen to water. The forests are directly grown by Chemical Vapor deposition on a conductive tantalum layer which provide enough mechanic stability during several functionalization and enzyme immobilization steps. A pyrene bis-anthraquinone derivative (Pyr-$(AQ)_2$) was attached via π-stacking throughout the forest and was used as anchor molecule for oriented immobilization of laccase. This led to high-performance biocathodes for oxygen reduction via direct electron transfer with maximum current densities up to 0.84 mA cm^{-2} at 0.2 V vs Ag/AgCl. The morphological changes during the wet chemical processes were studied by Scanning Electron Microscopy (SEM) revealing cellular

patterning of the forest structure. Despite these changes, the forest remained attached and electrically connected to the tantalum layer. The resulting bioelectrodes performed with satisfying stabilities under constant discharge conditions and kept 75 % of its initial performances after one week.

KEYWORDS: Carbon Nanotube Forests, Functionalization, Laccase, Biocathode, Oxygen Reduction, Direct Electron Transfer.

1. INTRODUCTION

The challenges in the field of enzymatic bio-fuel cell (EBFC) engineering is the efficient loading and wiring of the biological catalysts, combined with a convenient environment for enzymes to keep their optimal electrocatalytic activity.

Within many other materials [1], Carbon nanotubes (CNTs) in different macroscopic shapes like buckypapers, fibres, or pellets [2,3] have demonstrated to be an efficient material for biocatalytic electrodes due to its excellent combination of enzyme wiring capacities and high electroactive surface area enabling efficient electron transfers with a great amount of biocatalysts [4,5]. CNT forests are supposed to have improved electron transfer rates in electrochemical setups [6] but are difficult to handle and to contact without destroying the initial forest morphology. For instance, Miyake *et al.* formed free-standing bioelectrocatalytic films by trapping enzymes via liquid shrinking of a CNT forest which were applied for a fructose biofuel cell [7]. Zloczewska *et al.* transferred vertically aligned CNT (forests) to ITO electrodes with epoxy glue and studied the electrocatalysis with laccase enzymes for direct and mediated electron transfers [8]. Also, Kihara *et al.* transferred CNT forests to glassy carbon electrodes before studying the immobilization and

wiring of hydrogenase [9]. An original approach was presented by Kwon *et al.* [10] who used CNT forests to form yarns with entrapped enzymes using a biscrolling method. This led to a biofuel cell textile design. In all of these works, the CNT forests were removed from the growth substrate to form the bioelectrodes, because the CNTs forests were grown on non-conductive substrates and thus were not electrically contacted. Another reason is the little adhesion of the CNTs to the support leading to little mechanical stability.

Generally, CNT forest are grown on metal catalyst at high temperature using carbon precursor at high temperatures [11]. The nanoscale metallic catalyst particles, typical Fe, Co or Ni, are usually support on oxide supports, such as SiO_2 or Al_2O_3 [12].

An alternative approach was proposed by Żelechowska *et al.* with direct growth of curly CNT forests on graphite [13]. After removal of catalysts with nitric acid, these CNT layers were covalently functionalized with naphthalene using the diazonium strategy to immobilize the enzyme bilirubin oxidase. The obtained electrochemical oxygen biosensors revealed direct electron transfer with the enzyme. Further (bio)-functionalization strategies for vertically aligned CNTs are based on covalent grafting or via polymer coating of the desired entities on either the CNT forest tips or the whole forest including the sidewalls [14]. In this work, we synthesized CNT forests on a conducting tantalum layer which shows enough stability for non-covalent functionalization via dip coating using a pyrene derivative dissolved in organic media. Pyrene functionalization of carbon nanotubes via dip coating became a reliable method and we considered it as most appropriate for fragile systems like CNTs forests since it can be performed under ambient conditions without the need for mechanical stirring [15]. The use of an organic solvent allowed the diffusion and immobilization of a specific pyrene-based anchor function throughout the hydrophobic CNT forest to immobilize and wire the enzyme Laccase.

Laccase belongs to the multicopper oxidoreductase family and is a common cathodic biocatalyst in biofuel cell designs [16].

Since the original immobilization strategy proposed by Armstrong et al., which exploit the hydrophobic domain close to the T1 centre to immobilize and orientate the enzyme on anthracene modified surfaces establishing direct electron transfers [17], many similar approaches have been reported using e.g. naphthalene [18], anthraquinone [19], adamantane [20], and pyrene [21], making Laccase one of the mostly used cathodic enzyme in biofuel cells. To optimize the availability of such anchor function, we designed 1-[bis(2 anthraquinoyl)aminomethyl] pyrene (pyr-$(AQ)_2$) and improved the performance of CNT-based biocathodes [22]. This reliable immobilization and wiring strategy were used to study contacted CNT forests as potential biocatalytic electrode material. The anchor function for laccase, pyr-$(AQ)_2$, was attached to the CNT forest walls by the mentioned dip coating technique. In a second step, the complete removal of not-immobilized pyr-$(AQ)_2$ and solvent must be assured using different washing steps before the immobilization of Laccase in buffer solution to obtain the final biocathode. The morphological changes during the wet chemical processes were studied by Scanning Electron Microscopy (SEM) and the electrocatalytic performances of this setup were determined with cyclic voltammetry and chronoamperometry.

2. MATERIAL and METHODS

2.1. Materials

All reagents were purchased from Aldrich. Laccase (120 Umg^{-1}) from *Trametes versicolor* was purchased from Aldrich and stored at 4°C.

2-(bis(methylpyrenyl)aminomethyl)anthraquinone (**pyr-$(AQ)_2$**) was synthesized as described in [22]. In brief: 2-bromomethyl-anthraquinone (150 mg, 0.50 mmol), potassium carbonate (152 mg, 1.10 mmol) and (pyren-1-yl) methylamine (51 mg, 0.22 mmol) were dissolved in acetonitrile (30 mL). The mixture was stirred at 60 °C for 24 h under argon. After cooling to room temperature and removing of solvent by vacuum, the reaction mixture was diluted with CH_2Cl_2 and successively washed with water and HCl 0.1 M. The organic phase was dried over $MgSO_4$ and the solvent was evaporated. Purification by column chromatography on silica gel using dichloromethane as eluent gave the product as a yellow solid.

2.2. CNT forest growth*:*

The CNT forests were grown by CVD in a quartz tube furnace (Gero GmbH, Germany) as follows. The catalyst substrate was a 3 nm layer of CoFe (ratio of 90:10, respectively) on a layer of Ta (30 nm) deposited by PVD on a SiO_2 wafer (Si-Mat). The Ta layer ensured that the CNTs were connected to a conductive substrate. Catalyst samples were introduced to the furnace at 750° C and pure H_2 was initially flowed for 10 minutes at 60 sccm with a chamber pressure of 10 torr (maintained by a throttle valve on the exhaust) to condition the catalyst surface. Subsequently, C_2H_2 and Ar were introduced to the chamber (120 sccm, each) while maintaining H_2 flow, and the pressure was increased to 20 torr. This was maintained for 15 minutes of growth before shutting off all process gas flows. Samples were cooled under N_2 flow before removing from the growth furnace.

2.3. Preparation of bioelectrodes:

All functionalization and washing steps were performed in a "*plate material evaluating cell*" (ALS Japan, product no. 011951). Its containing nitrile 'O' ring defined the CNT forest working electrode surface area of 0.45 cm^2. In this cell, the CNT forests could be carefully immersed with the different liquids with a purge tube (ALS 010537). The CNT forests were firstly treated in a NMP solution containing pyr-$(AQ)_2$ (1 mg mL^{-1}) and subsequently washed with NMP and then with phosphate buffer saline (PBS, 0.1 $molL^{-1}$, pH 5.0). The functionalized electrodes were then immersed in a 5 mg mL^{-1} solution of laccase from *Trametes versicolor*, stored at 4°C in PBS for 48h, and washed with PBS. It has to be noted that until storage at 4°C in PBS, the electrodes were not allowed to dry.

This "*plate material evaluating cell*" was also used to perform the electrochemical measurements with a conventional three-electrode configuration by using an Autolab pgstat100 potentiostat and 0.1 $molL^{-1}$ PBS, pH 5.0 as supporting electrolytes in aqueous media at room temperature after purging the solution with Ar. The functionalized CNT forests, grown on tantalum, were used as the working electrode with a Pt counter electrode (ALS 002222), and an Ag/AgCl/Saturated KCl reference electrode (ALS **013691** RE-1CP). Pyr-$(AQ)_2$ was synthesized according to [22]. Field Emission-Scanning Electron Microscopy (FE-SEM) images were acquired using ULTRA 55 FESEM 176 based on the GEMINI FESEM column with beam booster (Nanotechnology Systems Division, 178 Carl Zeiss NTS GmbH, Germany) and tungsten gun.

3. RESULTS and DISCUSSION

3.1. Morphology studies

The pristine and modified CNT forests were characterized with SEM. At the top view (Figure 1A), the as-grown CNT forest shows a random entangled morphology without a clearly patterned array of tips. At the side view, a high density of slightly curled and straight vertically aligned

CNTs up to a length of 60 µm can be identified (Figure 1B). The multiwalled CNTs have diameter averaging around 10 nm und their density ranges about 10^{11} cm^{-2} , typically for CNT forest growth [23].

After the dip coating of nanotube forests with pyrene-AQ_2 and the immobilization of laccase, the CNT forest forms a cellular structure (Figure 1C) with compacted CNTs in some areas. N. Chakrapani *et al*. studied in detail this effect and related this phenomenon to capillary forces arising during the evaporation of liquids from CNT forests, which causes such changes of morphology [24]. A zoom at the side view (Figure 1D) gives more insight in this capillary effect, resulting in CNT tips sticking together in triangular shapes. Despite this structural change, the nanotube forest remains globally stable on the tantalum layer and the individual CNTs are homogeneously covered with a thin pyrene-$(AQ)_2$-laccase film. It can be suggested that such pattern formation might be related to the hydrophilic coating and that this allows an improved access of the enzymatic substrate (O_2, dissolved in buffer) to the biocatalyst in a mesoporous carbon environment [25].

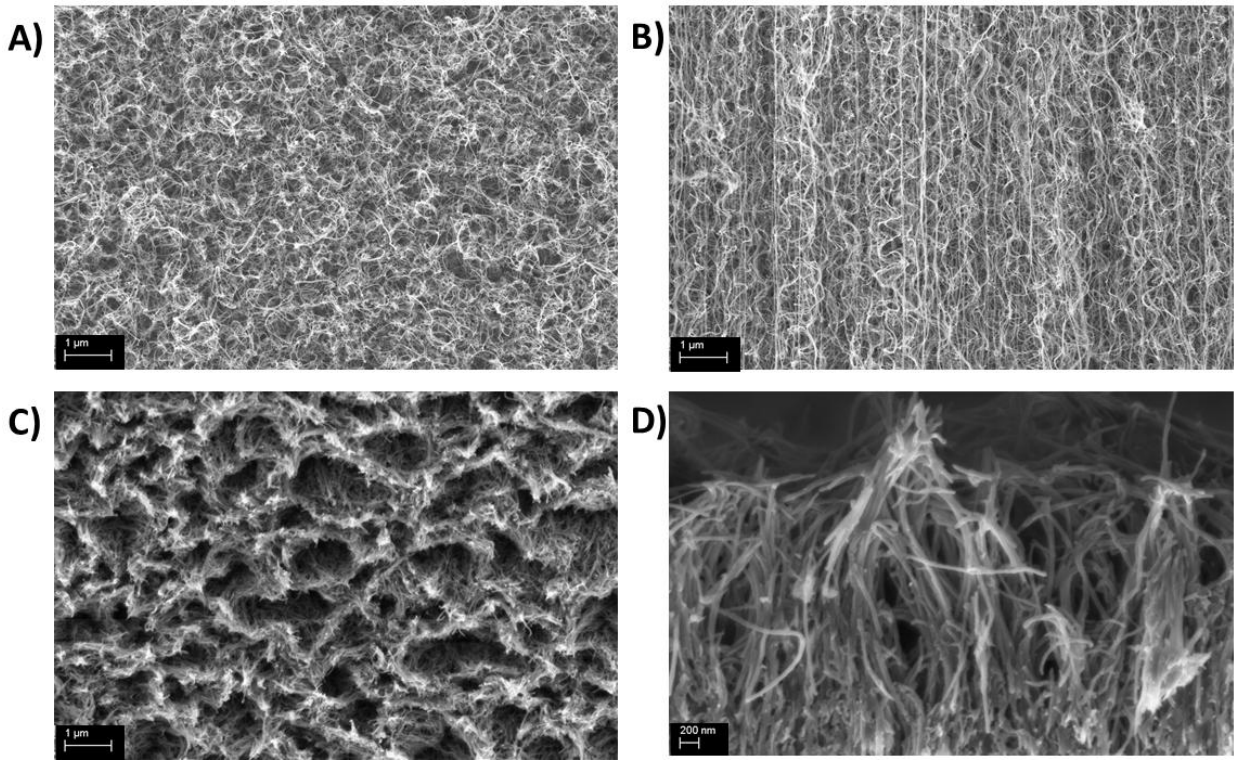

Figure 1: SEM images of A) top view of unmodified CNT forests, B) side view of unmodified CNT forests, C) top view of functionalized CNT forest bioelectrodes, and D) side view of functionalized CNT forest bioelectrodes.

3.2. Electrochemical studies and evaluation of the bioelectrocatalytic properties

We hypothesized that the functionalization of CNTs with a dip coating process is particularly appropriate for these CNT forests, since it barely affects the forest layer [15]. To demonstrate the suitability of this technique, electrochemical methods were used to validate the efficient functionalization of the forests with the electroactive pyrene-$(AQ)_2$. The cyclic voltammograms of unmodified and anthraquinone-functionalized CNT forest electrodes were recorded between -0.75 and 0.0 V in 0.1 M PBS electrolyte (Figure 2).

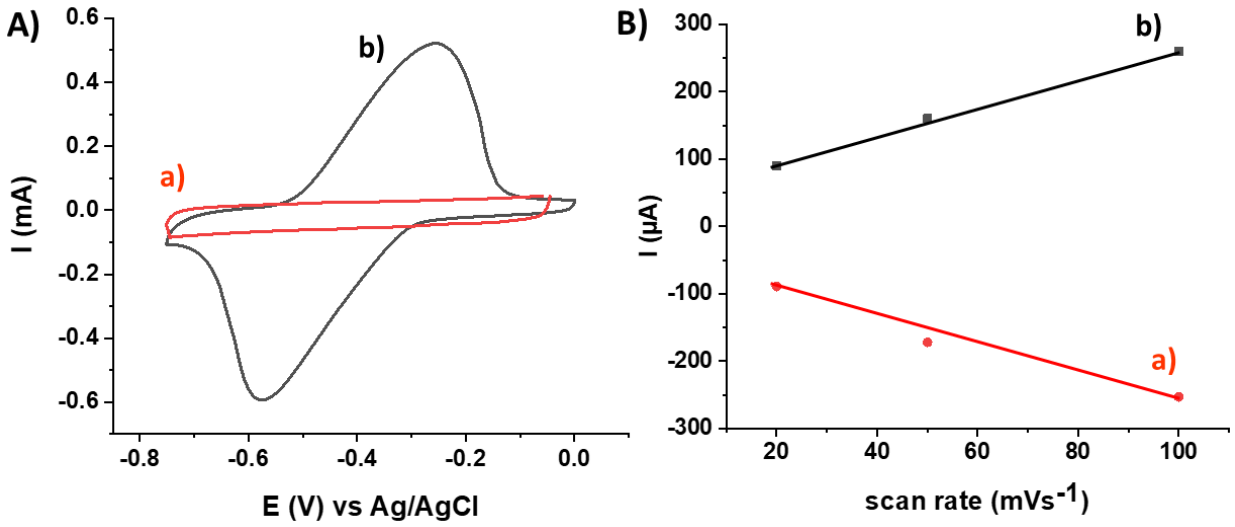

Figure 2. A) Cyclic voltammograms between -0.75 and 0.0 V of pristine CNTforests (a) and nanotube pyrene$(AQ)_2$ functionalized forests (b) in PBS 0.1 mol L^{-1} (pH 5). Scan rate v = 0.02 V s^{-1}. B) plot of cathodic (a) and anodic (b) peak currents as a function of the scan rate (20, 50, 100 mVs^{-1})

One reversible redox system was observed at $E_{1/2}$ = - 0.41 V for the pyrene-$(AQ)_2$ modified forests while the untreated forests showed no electrochemical features in this potential range. As previously reported for the electrochemical behaviour of anthraquinone derivatives in water [26], this couple corresponds to the $2H^+/2e^-$ reduction of immobilized anthraquinone groups (equation 1)

$$AQ + 2e + 2H^+ \rightarrow AH_2Q, \quad (1)$$

where AQ and AH_2Q are the oxidized (quinone) and reduced (hydroquinone) form, respectively. A relatively high peak separation of ΔEp = 0.32 V was observed, which can be attributed to a slow diffusion of the electrolyte through the modified forests.

To verify the efficiency of this functionalization strategy, cyclic voltammograms were recorded at different scan rates. Figure 2 B) shows the plot of the anodic and cathodic maximum currents at 20, 50, and 100 mVs^{-1}. The cathodic and anodic current evolution was nicely linear with an average coefficient R^2 of 0.989 demonstrating the stable immobilization of the anthraquinone units on the CNT forests.

To investigate the appropriateness of these functionalized CNT forests for bioelectrocatalytic applications, unmodified and pyr-$(AQ)_2$-functionalized forest were modified with laccase and the bioelectrocatalytic activity of the electrodes towards the reduction of dioxygen was studied by cyclic voltammograms recorded under argon and oxygen purging (Figure 3).

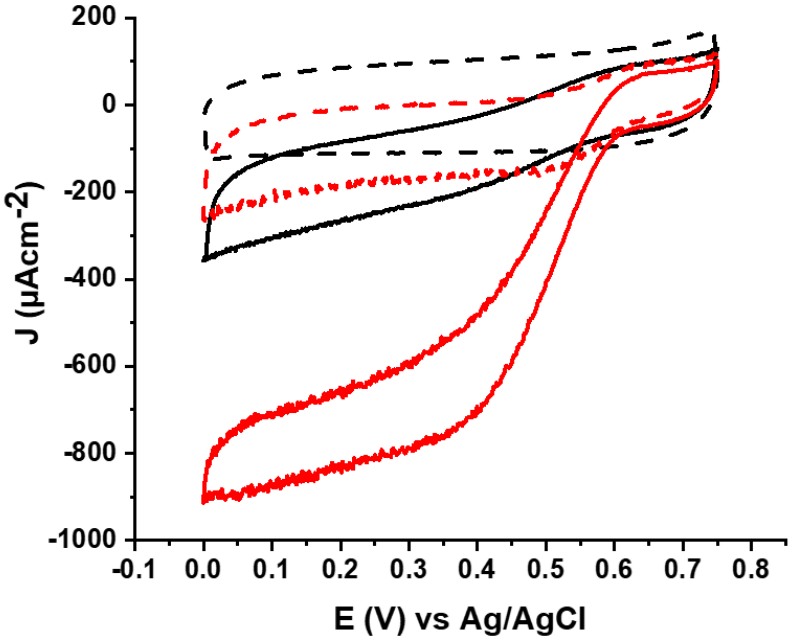

Figure 3: Cyclic voltammograms of laccase-functionalized CNT forest electrodes. a) CNT forests/Lac under argon (in black, dotted), b) CNT forests/Lac under oxygen (in black, continuous) and c) CNT forests/ pyr-$(AQ)_2$/Lac under argon (in red, dotted) d) CNT forests/ pyr-$(AQ)_2$/Lac under oxygen (in red, continuous) in 0.1molL^{-1} PBS (pH 5.0); scan rate v= 0.01 V^{-1}.

The unmodified CNT forests and anthraquinone-functionalized CNT forests were compared towards their catalytic oxygen reduction current. CV scans were performed for the two electrodes under Ar and constant O_2 flow. Under argon, no electrocatalytic activity was observed for the untreated laccase electrodes but we observed a small electrocatalytic wave for the pyr-$(AQ)_2$ laccase electrodes which is most likely due to the presence of oxygen residues in the forest. Under O_2 purging, both electrodes exhibited an onset potential of 0.58 V, closely matching the redox potential of the *Trametes versicolor* T1 centre of laccase [27]. All these electrodes displayed an electrocatalytic reduction wave, confirming direct electron transfer (DET) between CNT forests and laccase. These catalytic currents account for the electrocatalytic properties of directly wired laccase on the CNT forests surface. When the CNT forest was first incubated with pyr-$(AQ)_2$, the maximum current density increased approximately three times compared to laccase randomly adsorbed on CNT forests (0.26 mA cm^{-2}), reaching 0.84 mA cm^{-2} at 0.2 V. This drastic improvement cannot only be explained by the efficient orientation and wiring strategy using pyr-$(AQ)_2$, but also by a hydrophobic character of unmodified the CNT forests. Since Laccase containing buffer solutions do not penetrate the forest, only the surface of the forest could be modified with laccase. In contrast, initial modification with pyr-$(AQ)_2$, dissolved in DMF allows the access throughout the forest structure and forms the discussed cellular structure (Figure 1 C, D). The resulting CNT forest provides an improved wettability resulting in better diffusion of aqueous Laccase and, later, oxygen containing buffer solution. With this morphology change, the forest CNTs appear also more accessible for enzyme functionalization.

In comparison with similar approaches, Zloczewska *et al.* employed vertically aligned CNT forest film electrodes for bioelectrocatalytic dioxygen reduction and found very high non-

mediated catalytic dioxygen reduction current 400 μA cm^{-2} using VACNTs functionalized with 1-pyrenesulfonic acid [8]. Here, we unambiguously confirm the major role of anthraquinone to guide the enzyme efficiently on the electrode surface by interacting with the hydrophobic pocket near the T1 copper centre.

We also investigated the operational stability of the forest electrodes by performing one-hour discharge at 0.3 V using chronoamperometry (Figure 4A). The CNT forest functionalized with pyr-$(AQ)_2$ and laccase exhibited excellent stability under continuous discharge. The observed fluctuation of the discharge current can be explained by the constant O_2 bubbling during the experiment. Furthermore, by storing the electrodes in buffer solution at 5°C, just a 25 % loss of the catalytic activity for MWCNT/pyr-$(AQ)_2$/Lac electrode was observed after 7 days (Figure 4 B). The decrease likely arises from desorption of both weakly adsorbed pyrene molecules or enzymes.

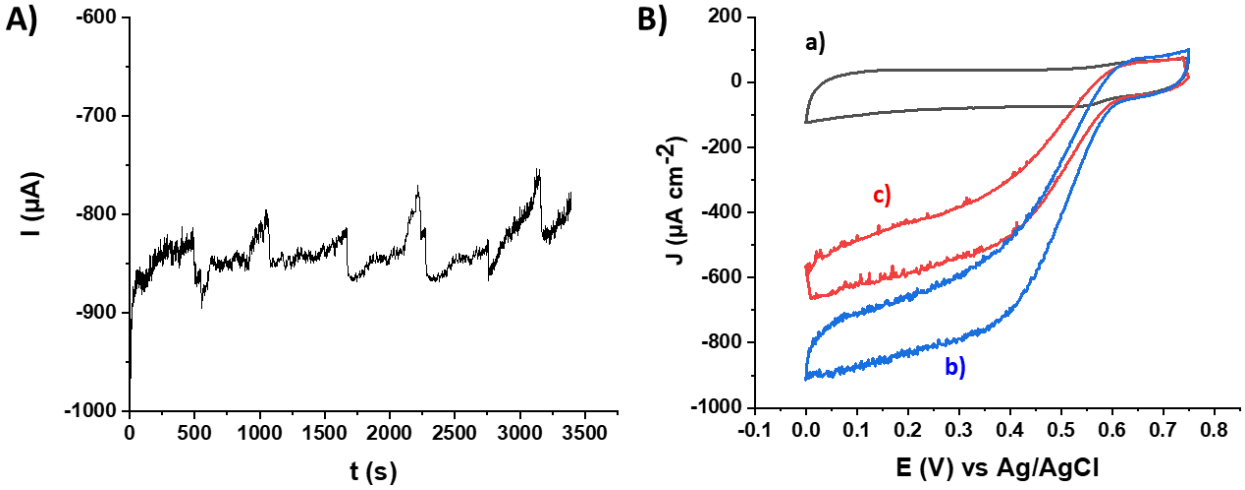

Figure 4. A) Chronoamperometric response for a CNT forest/pyr-$(AQ)_2$/Lac. E_p = 0.3 V (vs $Ag/AgCl_{sat}$) in 0.1 molL^{-1} PBS solution (pH 5.0) under constant oxygen bubbling. B) Cyclic voltammograms of laccase-functionalized CNT forest electrodes. a) CNT forests/Lac under argon, b) CNT forests/ pyr-$(AQ)_2$/Lac under oxygen, and c) CNT forests/ pyr-$(AQ)_2$/Lac under oxygen after one-week storage in 0.1 molL^{-1} PBS (pH 5.0); scan rate v= 0.01 V s^{-1}.

4. CONCLUSIONS

In this work, we introduced a novel functionalization strategy for CNT forests. Contacted CNT forests were functionalized with Laccase to form stable electrocatalytic bioelectrodes without removing from the substrate. Our results showed that dip coating of pyrene derivatives represents the smoothest functionalization method, which just slightly alters the forest structure. The supramolecular functionalization of vertically aligned CNT forests allowed the oriented immobilization of the multicopper enzyme Laccase. As such, high performing biocathodes with direct electron transfer between the enzyme and the connected CNT forests could be formed This novel CNT forests functionalization strategy makes this material competitive in terms of bioelectrocatalytic performances and stabilities with classic CNT layers on electrodes for biofuel cell applications.

ACKNOWLEDGMENT

The authors would like to thank the French–Canadian Research Found (FCRF) for the Ph.D. fellowship for MS. The authors also acknowledge the support from the platform Chimie NanoBio ICMG FR 2607 (PCN-ICMG), from the LabEx ARCANE (ANR-11-LABX-0003-01 and CBH-EUR-GS, ANR-17-EURE-0003), and from the Institut Carnot PolyNat (CARN 0007-01). GSD and HN thank Science Foundation Ireland under SFI-PI15/IA/3131

DATA AVAILABILITY

The raw/processed data required to reproduce these findings cannot be shared at this time due to technical or time limitations. All experimental details for the reproduction of this work can be found in the Material and Methods section

REFERENCES

1. Zhu, Z., *Nanomicro Lett* (2017) **9** (3), 25. doi: 10.1007/s40820-017-0128-6
2. Holzinger, M., Haddad, R., Le Goff, A., Cosnier, S., Enzymatic Glucose Biofuel Cells: Shapes and Growth of Carbon Nanotube Matrices. In *Dekker Encyclopedia of Nanoscience and Nanotechnology*, *Third Edition*, Lyshevski, S. E., (ed.) CRC Press(2016), pp 1-10
3. Kumar, A., Sharma, S., Pandey, L. M., Chandra, P., *Materials Science for Energy Technologies* (2018) **1** (1), 38-48. doi: 10.1016/j.mset.2018.04.001
4. Holzinger, M., Le Goff, A., Cosnier, S., *Electrochim. Acta* (2012) **82**, 179–190. doi: 10.1016/j.electacta.2011.12.135
5. Gross, A. J., Holzinger, M., Cosnier, S., *Energy Environ. Sci.* (2018) **11** (7), 1670-1687. doi: 10.1039/c8ee00330k
6. Miller, T. S., Ebejer, N., Guell, A. G., Macpherson, J. V., Unwin, P. R., *Chem Commun (Camb)* (2012) **48** (60), 7435-7437. doi: 10.1039/c2cc32890a
7. Miyake, T., Yoshino, S., Yamada, T., Hata, K., Nishizawa, M., *J. Am. Chem. Soc.* (2011) **133** (13), 5129–5134. doi: 10.1021/ja111517e
8. Zloczewska, A., Jönsson-Niedziolka, M., Rogalski, J., Opallo, M., *Electrochim. Acta* (2011) **56** (11), 3947-3953. doi: 10.1016/j.electacta.2011.02.021
9. Kihara, T., Liu, X.-Y., Nakamura, C., Park, K.-M., Han, S.-W., Qian, D.-J., Kawasaki, K., Zorin, N. A., Yasuda, S., Hata, K., Wakayama, T., Miyake, J., *International Journal of Hydrogen Energy* (2011) **36** (13), 7523-7529. doi: 10.1016/j.ijhydene.2011.03.135
10. Kwon, C. H., Lee, S.-H., Choi, Y.-B., Lee, J. A., Kim, S. H., Kim, H.-H., Spinks, G. M., Wallace, G. G., Lima, M. D., Kozlov, M. E., Baughman, R. H., Kim, S. J., *Nat Commun* (2014) **5**, 3928. doi: 10.1038/ncomms4928
11. Duesberg, G. S., Graham, A. P., Kreupl, F., Liebau, M., Seidel, R., Unger, E., Hoenlein, W., *Diamond and Related Materials* (2004) **13** (2), 354-361. doi: 10.1016/j.diamond.2003.10.021
12. Graham, A. P., Duesberg, G. S., Seidel, R. V., Liebau, M., Unger, E., Pamler, W., Kreupl, F., Hoenlein, W., *Small* (2005) **1** (4), 382-390. doi: 10.1002/smll.200500009

13. Żelechowska, K., Trawiński, B., Dramińska, S., Majdecka, D., Bilewicz, R., Kusz, B., *Sensors and Actuators B: Chemical* (2017) **240**, 1308-1313. doi: 10.1016/j.snb.2016.09.081
14. Van Hooijdonk, E., Bittencourt, C., Snyders, R., Colomer, J. F., *Beilstein J Nanotechnol* (2013) **4**, 129-152. doi: 10.3762/bjnano.4.14
15. Holzinger, M., Baur, J., Haddad, R., Wang, X., Cosnier, S., *Chem. Commun.* (2011) **47** (8), 2450–2452. doi: 10.1039/c0cc03928d
16. Le Goff, A., Holzinger, M., Cosnier, S., *Cell. Mol. Life Sci.* (2015) **72** (5), 941-952. doi: 10.1007/s00018-014-1828-4
17. Blanford, C. F., Heath, R. S., Armstrong, F. A., *Chemical Communications* (2007) **0** (17), 1710-1712. doi: 10.1039/B703114A
18. Karaśkiewicz, M., Nazaruk, E., Żelechowska, K., Biernat, J. F., Rogalski, J., Bilewicz, R., *Electrochemistry Communications* (2012) **20** (0), 124-127. doi: 10.1016/j.elecom.2012.04.011
19. Lalaoui, N., Le Goff, A., Holzinger, M., Mermoux, M., Cosnier, S., *Chem. Eur. J.* (2015) **21** (8), 3198-3201. doi: 10.1002/chem.201405557
20. Lalaoui, N., David, R., Jamet, H., Holzinger, M., Le Goff, A., Cosnier, S., *ACS Catal.* (2016) **6** (7), 4259-4264. doi: 10.1021/acscatal.6b00797
21. Lalaoui, N., Elouarzaki, K., Le Goff, A., Holzinger, M., Cosnier, S., *Chemical Communications* (2013) **49** (81), 9281-9283. doi: 10.1039/C3CC44994G
22. Bourourou, M., Elouarzaki, K., Lalaoui, N., Agnès, C., Le Goff, A., Holzinger, M., Maaref, A., Cosnier, S., *Chemistry* (2013) **19** (28), 9371-9375. doi: 10.1002/chem.201301043
23. Yang, J., Esconjauregui, S., Robertson, A. W., Guo, Y., Hallam, T., Sugime, H., Zhong, G., Duesberg, G. S., Robertson, J., *Applied Physics Letters* (2015) **106** (8), 083108. doi: 10.1063/1.4913762
24. Chakrapani, N., Wei, B., Carrillo, A., Ajayan, P. M., Kane, R. S., *Proceedings of the National Academy of Sciences* (2004) **101** (12), 4009. doi: 10.1073/pnas.0400734101
25. Tsujimura, S., Kamitaka, Y., Kano, K., *Fuel Cells* (2007) **7** (6), 463-469. doi: 10.1002/fuce.200700032

26. Sosna, M., Stoica, L., Wright, E., Kilburn, J. D., Schuhmann, W., Bartlett, P. N., *Phys. Chem. Chem. Phys.* (2012) **14** (34), 11882-11885. doi: 10.1039/C2CP41588G

27. Blanford, C. F., Foster, C. E., Heath, R. S., Armstrong, F. A., *Faraday Discussions* (2009) **140** (0), 319-335. doi: 10.1039/B808939F